Title

Activation Effect of Electrochemical Cycling on Gold Nanoparticles towards the Hydrogen Evolution Reaction in Sulfuric Acid

Authors

Wang, Ying
Sun, Yuanmiao
Liao, Hanbin
et al.

Publication Date

2016-08-01

DOI

10.1016/j.electacta.2016.05.095

Peer reviewed

Electrochimica Acta 209 (2016) 440–447

Contents lists available at ScienceDirect

Electrochimica Acta

journal homepage: www.elsevier.com/locate/electacta

Activation Effect of Electrochemical Cycling on Gold Nanoparticles towards the Hydrogen Evolution Reaction in Sulfuric Acid

Ying Wang[a,b], Yuanmiao Sun[a], Hanbin Liao[a,b], Shengnan Sun[a], Shuzhou Li[a], Joel W. Ager III[c,d], Zhichuan J. Xu[a,b,d,e,*]

[a] School of Materials Science and Engineering, Nanyang Technological University, 50 Nanyang Avenue, 639798, Singapore
[b] Solar Fuels Lab, Nanyang Technological University, 50 Nanyang Avenue, 639798, Singapore
[c] Department of Materials Science and Engineering, University of California at Berkeley, Berkeley, California 94720, USA
[d] Singapore-Berkeley Research Initiative for Sustainable Energy, 1 Create Way, 138602, Singapore
[e] Energy Research Institute@NTU, Nanyang Technological University, 50 Nanyang Avenue, 639798, Singapore

ARTICLE INFO

Article history:
Received 15 February 2016
Received in revised form 24 March 2016
Accepted 14 May 2016
Available online 17 May 2016

Keywords:
electrocatalysis
gold
nanoparticles
hydrogen evolution reaction

ABSTRACT

This article reports a study of electrochemical cycling effects on hydrogen evolution catalytic activity of gold nanoparticles in sulfuric acid. We found that after cycling within the double layer regime, up to 0.64 V vs RHE, there is a dramatic effect on the HER activity of gold nanoparticles: 128 mV drop of the overpotential, a decrease of 23 mV/dec for the Tafel slope as well as a nearly twenty times increase of the turn-over frequency (TOF). This enhanced activity is tentatively assigned to the formation of stepped like structures by the consecutive electrochemical cycling in the double layer region.

1. Introduction

To sustainably consider the globally rapid increasing demand of energy, tremendous efforts are being devoted to advance the technologies for clean and renewable energy conversion [1–11]. Among these green energy approaches, the hydrogen evolution reaction (HER) is attracting significant attention due to its role in electrochemical water splitting and the subsequent use of the generated hydrogen in fuel cells [9,11–13].

In the classic HER reaction model, the first reaction always involves an intermediate of adsorbed hydrogen atoms on the electrode surface, which is the Volmer step shown in Eq. (1). It is followed either by the Tafel step (Eq. (2)) or the Heyrovsky step (Eq. (3)) depending on the nature of the electrode material [1,2,6,8–10,14,15].

$$H^+(aq) + e^- \rightarrow H^* \text{ (Volmer)} \quad (1)$$

$$2H^* \rightarrow H_2 \text{ (gas) (Tafel)} \quad (2)$$

or,

$$H^+(aq) + H^* + e^- \rightarrow H_2 \text{ (gas) (Heyrovsky)} \quad (3)$$

*surface adsorbed species

A good catalyst for HER should increase the process efficiency by minimizing the overpotential required. Due to the nature of this adsorptive mechanism, the catalyst is required to possess the ability to form a sufficiently strong bond with H* to further the proton reduction while a weak enough bond to assure release of the gas phase hydrogen from the electrode surface [9]. This is also described in the classic volcano plot by Nørskov which presents the correlation of exchange current density with the adsorption energy of H* [16]. By this analysis, gold is a poor catalyst for the HER due to the weak bond with H*.

Here, we employ continuous electrochemical cycling with different upper limit cycling potentials to "modify" 10 nm gold nanoparticles (Au-NPs) modified glassy carbon electrodes (Au-NPs/GCE) and then investigate the HER activity in 0.5 M sulfuric acid. This electrochemical cycling method is commonly used by researchers to electrochemically polish/clean gold electrodes surface [17,18]. It consists of two steps with the initial oxidation

* Corresponding author. Tel.: +65 6592 3170.
E-mail address: xuzc@ntu.edu.sg (Z.J. Xu).

http://dx.doi.org/10.1016/j.electacta.2016.05.095
0013-4686/

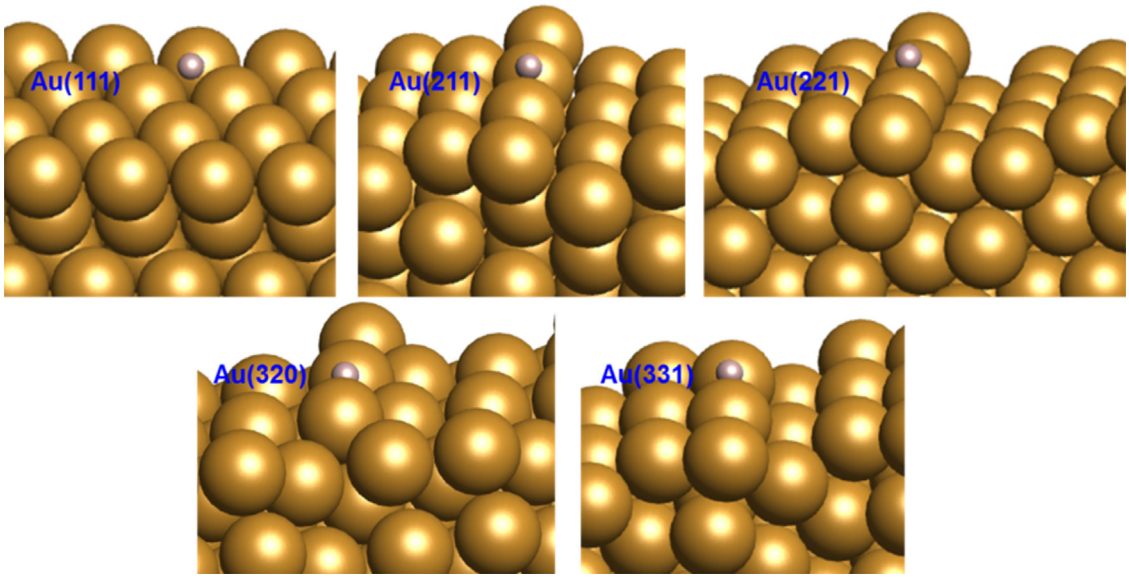

Fig. 1. Side view of the most stable binding configuration of H chemisorption (pink dot) on plane and stepped Au surfaces.

of gold in the forward scan and the reduction process to metallic gold in the reverse scan. By repetitively applying this process, the gold electrode is believed to go through an "electrochemical polishing" procedure, therefore, to reach a "refreshed" surface. However, it is also widely accepted that this electrochemical cycling process will cause surface atom reorientation and/or changes of the metal-solution interface [19,20], thus, altering electrochemical behavior to some inner-sphere electron transfer processes like oxygen reduction reaction [18] and CO oxidation [20]. Consequently, considering the nature of the HER, the electrochemical cycling process might also have an influence on the electrochemical response of the gold surface. Through this work, we study this hypothesis and investigate the cycling effect on HER.

2. Experimental

2.1. Electrochemical Experiments

The gold nanoparticles employed in this work was synthesized by mixing 100 mg $HAuCl_4{\cdot}xH2O$ (>99%, Sigma-Aldrich) with 10 mL1-Octadecene (>90%, Sigma-Aldrich) and 10 mL oleylamine (>70%, Sigma-Aldrich) under 120 °C for 45 minute. The surfactants of the gold nanoparticles were removed by burning at 250 °C for 30 min in box furnace under air condition. Then "ink" of 2 mg/mL was prepared in ethanol with 20% wt of surfactant removed gold nanoparticles and carbon black (GasHub Technology, Singapore). Prior to the electrochemistry measurement, 5 μL of the as-prepared "ink" was drop-casted on to a glassy carbon macro electrode and dried under lab atmosphere. All the solutions were prepared using Milli-Q water (18 MΩ·cm).

All the electrochemical experiments were carried out with SP-150 potentialstat (Bio-Logic SAS, France) under the room temperature. A platinum wire was employed as the counter electrode and a saturated calomel electrode (SCE, Tianjin Aida Hengsheng Technology Development Co. Ltd, China) was used as the reference electrode. All the results reported in this work have been converted to the reversible hydrogen electrode. A bare or modified glassy carbon electrode (GCE, 5 mm diameter, Tianjin Aida Hengsheng Technology Development Co. Ltd, China) or a bare gold macro-electrode (Au, 3 mm diameter, Tianjin Aida Hengsheng Technology Development Co. Ltd, China) was employed as working electrode. The glassy carbon electrode was polished with 0.05 μm alumina lapping compounds (Tianjin Aida Hengsheng Technology Development Co. Ltd, China) for 20 minutes and sonicated in an ultrasound bath prior to use. The amount of the hydrogen was determined from the gaseous product in the headspace of the sealed cell using gas chromatography (Agilent 7890 A) with TCD detector.

2.2. First Principle Calculation

The density functional theory (DFT) calculations were carried out by using the Vienna Ab-initio simulation package [21] with the projector augmented wave [22]. The revised Perdew–Burke–Ernzerhof [23] was chosen to describe the electron exchange and correlation effects. An energy cut-off of 350 eV was used for plane wave basis expansion. The electronic relaxation was carried out by applying the Monkhorst-Pack [24] grids of $3 \times 3 \times 1$ k-points and the convergence criterion of the electronic self-consistent field iteration was set to be 10^{-5} eV.

The electronic binding energy was calculated as the difference between the bonding system and the clean slab together with the adsorbate,

$$\Delta E_H = E_{slab+H} - E_{slab} - 1/2E_{H2}$$

Where, E_{slab+H} is the total energy of the H bonding system, E_{slab} is the electronic energy of the slab and E_{H2} is the energy of gas phase hydrogen molecule. The configuration of the most stable binding system and the corresponding binding energy are shown in Fig. 1 and Table 1, respectively.

Table 1
H binding energy and bond length on plane and stepped Au surfaces.

Surface	Au(111)	Au(211)	Au(221)	Au(320)	Au(331)
$d_{H\text{-}Cu}$ (Å)	1.89	1.78	1.79	1.77	1.78
Binding energy (eV)	0.25	0.08	0.17	0.12	0.14

Table 2
Zero point energy of H chemisorption on plane and stepped Au surfaces.

Surface	Au(111)	Au(211)	Au(221)	Au(320)	Au(331)
Zero point energy (eV)	0.13	0.15	0.15	0.16	0.15

The H chemisorption free energy was then calculated by adding the zero point energy and entropy corrections to the electronic binding energy, which can be defined as following

$$\Delta G_{H*} = \Delta E_H + \Delta E_{ZPE} - T\Delta S_H$$

Where, ΔE_H is the electronic binding energy, ΔE_{ZPE} is the difference of zero point energy between the adsorbed hydrogen atom and half the gaseous hydrogen molecule and ΔS_H is the corresponding entropy difference. The calculated zero point energy of gas phase hydrogen molecule in this work was 0.28 eV, in good agreement with the 0.27 eV value in reported publication [25]. The zero point energies of chemisorbed H atom on the perfect and stepped Au surfaces were summarized in Table 2. Taken into consideration that the entropy of an adsorbed H atom was very little and can be neglected [26], the entropy correction was treated as $\Delta S_H = 1/2\, S_{H2}$, where S_{H2} is the entropy of gaseous hydrogen molecule at standard conditions. The TS of 0.41 eV at 300 K of H_2 in the gas phase, taken from standard molecular Table [27], was applied in this work.

3. Results and Discussion

3.1. Electrochemical Cycling

The cyclic voltammetry (CV) of the Au-NPs/GCE in 0.5 M sulfuric acid is firstly examined. Fig. 2 shows CV scans using the different upper limit potential employed for this study, which ranged from the double layer region, where no faradaic current observed, (A: 0.64 V vs. RHE and B: 1.04 V vs. RHE) to the commonly used potential applied for the electrochemical polishing process (D: 1.74 V vs. RHE). Fig. 1.d shows the "fingerprint" of the 1st scan and 10th scan (dotted line) for the Au-NPs/GCE from 0.24 V until 1.74 V vs. RHE in argon saturated 0.5 M sulfuric acid solution at 298 K at a scan rate of 100 mVs^{-1}. Clearly, the oxidation process on Au-NPs/GCE initiates at around ca. 1.10 V with the formation of AuOH [28,29]. This is followed by further formation of gold oxide monolayers, like AuO or Au_2O_3 [18,28,30]. Application of a potential larger than 1.74 V vs RHE is avoided to prevent detachment of gold nanoparticles [31] from the electrode and aggressive growth of multi-oxide layers on the surface [28,32]. In the reverse scan, a major cathodic peak appears at 1.14 V vs. RHE corresponding to the reduction of gold oxide to metallic gold [18,30,33–35].

In the 10th scan in Fig. 2d, it can be observed that a small anodic peak (OA1) becomes more apparent compared to that in the 1st scan. The formation of this OA1 peak is complicated. Some reports [18,34,35] have associated it with an increase of the surface defects [36,37] while others suggest the electrodeposition of OH and O species on the anion free surface of the electrode [30,38]. In a paper by Compton [18], decreased electroactivity of the ORR was observed on gold nanoparticles with an increased intensity of this peak. They associated it with a possible poisoning effect resulting from an increased composition of surface defects generated in the cycling process. Here, we hypothesize that this OA1 process will also alter the electroactivity of gold nanoparticles towards the HER. Therefore, as shown in Fig. 2c, a upper limit potential of 1.39 V vs RHE, which is just after this process, is chosen in order to study the HER performance of Au-NPs/GCEs cycled with this potential.

3.2. The HER on the Au-NPs/GCEs after Electrochemical Cycling

A comparison of the HER performance on Au-NPs/GCEs cycling with A: 0.64 V (red line), B: 1.04 V (blue line), C: 1.39 V (green line), D: 1.74 V (purple line) and O: without cycling process (black line) in 0.5 M sulfuric acid at 100 mVs^{-1} and 298 K is shown in Fig. 3a. The

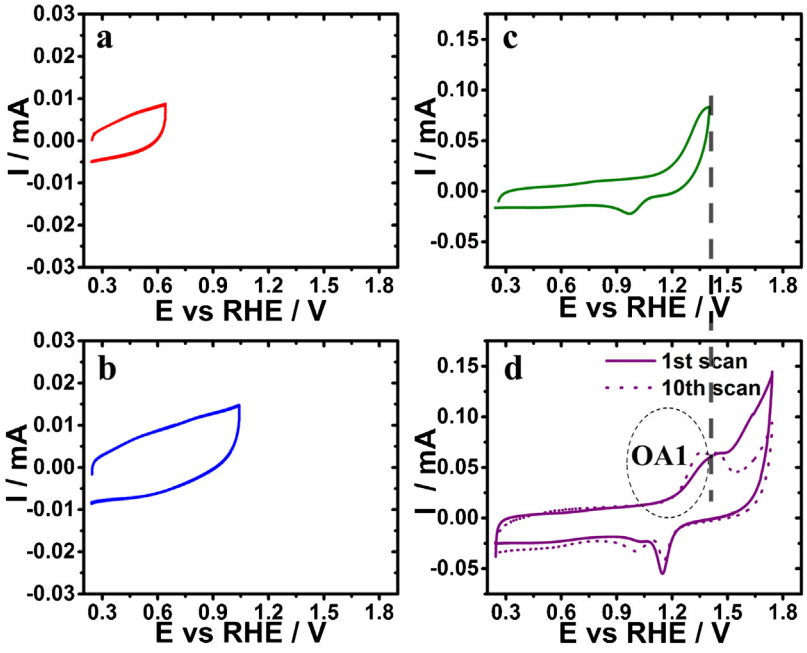

Fig. 2. Cyclic voltammery of the electro-chemical oxidation/reduction of Au-NPs/GCE with different upper limit potential: a. 0.64 V; b. 1.04 V; c. 1.39 V and d. 1.74 V in argon saturated 0.5 M sulfuric acid solution, 298 K, 100 mVs^{-1}.

current densities calculated here are based on the real surface area of gold nanoparticles, which is derived from the reduction peak of gold. Similar to the report by Sun et al. [39], when cycled in the double layer region, the onset potential of the HER shifts positively with the increased number of potential cycles; the results shown here are the steady value. A comparison of the overpotential, ($\eta = E_{onset} - E_0$, where E_{onset} is the potential when HER occurs, Eo is the standard potential of the HER), of the HER needed for Au-NPs/GCEs cycled under different potentials is made in the insert in Fig. 3a. As shown, the overpotentials of the HER reaction on the Au-NPs/GCEs after continuous cycling in the double layer regions (A and B) have considerable decreases in overpotentials of 125 mV and 99 mV, respectively, compared to those without cycling. This suggests a dramatic drop of the energy required in order to initiate the HER process. This electrocatalytic

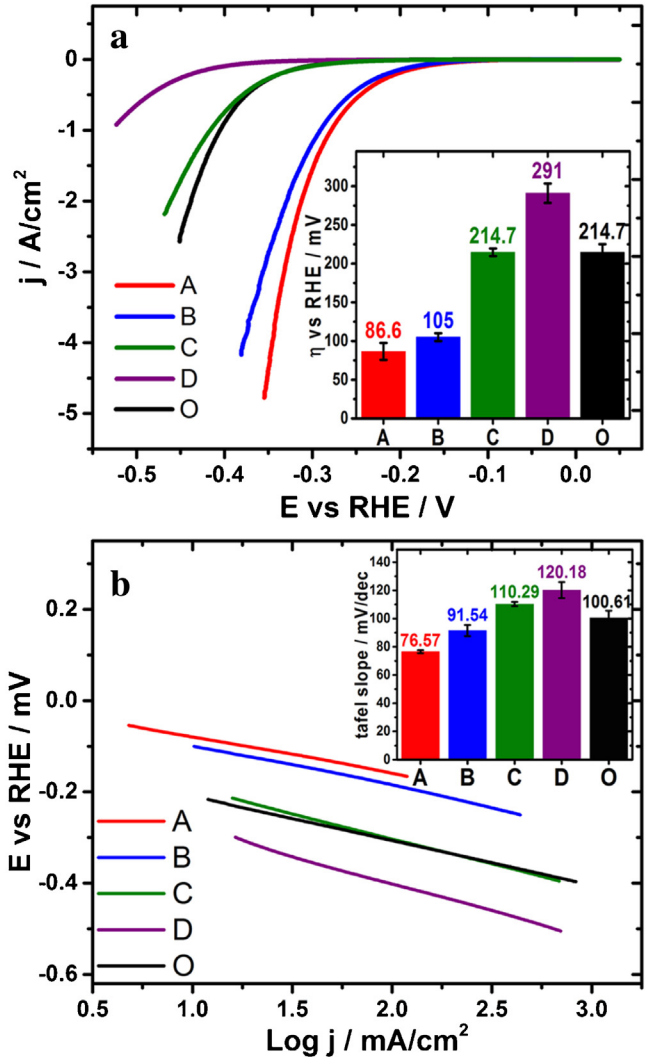

Fig. 3. (a).The HER in argon saturated 0.5 M sulfuric acid solution on Au-NPs/GCEs cycling with A: 0.64 V(red line), B: 1.04 V (blue line), C: 1.39 V (green line), D: 1. 74 V (purple line), and Original: without cycling (black line), 298 K, 100 mVs-1, and the insert is the comparison of overpotential needed for the HER on Au-NPs/GCEs after electrochemical cycling with different upper limit potential; (b) tafel analysis for hydrogen evolution reaction on Au-NPs/GCE treated with different upper limit potentials: 0.64 V (A, red line), 1.04 (B, blue line), 1.39 (C, green line), 1.74 (D, purple line) and Au-NPs/GCE without cycling (O, black line). The error bars are obtained by three independent measurements. (For interpretation of the references to color in this figure legend, the reader is referred to the web version of this article.)

activity is also suggested by the turn-over frequencies $\left(\text{TOF} = \frac{\#\text{total hydrogen turn overs/cm}^2\text{ geometricarea}}{\#\text{activesites/cm}^2\text{ geometricarea}}\right)$ [12] calculated at −0.35 V, as there is a nearly twenty times increase in the turnover frequencies for the Au-NPs/GCE under condition A ($4.43 \times 10^{-4}\,s^{-1}$) compared to those without cycling ($2.82 \times 10^{-5}\,s^{-1}$). On the other hand, it seems that the OA1 process has a minor effect towards the HER activity since the overpotentials and the shape of the voltammograms from Au-NPs/GCE cycled at an upper limit potential at 1.39 V vs RHE are similar to those without cycling. Nevertheless, a clear increase of the overpotential is found from Au-NPs/GCE cycled with upper limit potential at 1.74 V vs RHE, suggesting a more sluggish kinetics for HER compared to the rest.

The Tafel slope (shown in Fig. 3b) obtained from the Butler-Volmer equation [40] is analyzed to allow a further understanding of the results. This value for those Au-NPs/GCEs without cycling (O) is 100.6 ± 5.0 mV/dec, which is in agreement with literatures [41,42]. The smallest Tafel slope value of 76.6 ± 1.9 mV/dec was obtained on the Au-NPs/GCE cycled under condition A; this value is 23.4 mV smaller than for uncycled nanoparticles. This decrease of the Tafel slope indicates a faster adsorption of the H* on the cycled nanoparticles, and also suggests that the rate determining factor may not due to a single step [43]. The Tafel slopes for Au-NPs cycled under condition B and C are 91.5 ± 3.9 mV/dec and 110.3 ± 1.5 mV/dec, respectively. The most sluggish value of Tafel slope, 120.2 ± 5.7 mV/dec, is again obtained on the group D indicating that the Volmer step is the rate determining step in the HER process.

Although the HER activity is still not as good as Pt [44] due to the nature of the poor adsorption of H* on gold materials [26], a significant improvement of the performance is obtained through electrochemical cycling under varied "upper limit cycling potential". To explore the origins of this catalytic effect could be able to shed some lights on how to design catalysts for the HER in the future. It might be correlated with the complicated gold oxidation process in sulfuric acid which involves chemical adsorption, electro-oxidation, possible gold dissolution and a potential induced surface reconstruction process [18,28,30,31,33–37,45–50]. Based on the studies on the bulk gold electrode [46,51], under the condition A, a step like structure is believed to be formed with the "lifting" effect of some surface gold atoms from the change of surface energy due to specific adsorbed anions on the gold surface [52]. With the increasing of the upper limit potential to condition B, via STM, Kolb et al. observed that the step-like structures start to vanish due to the instability under higher potential [45] and these structures will be removed completely when the potential reaches the condition C. This reported phenomena correlates well with what we observed for the electrocatalytic effects for the HER on the Au-NPs/GCE and bulk Au (Fig. 4). However, the electrocatalytic effect seems to be more apparent on the nanoscale compared to the macro-scale, which might due to that there is more structural defects on the gold nanoparticles compared to the bulk material. We thus suspect that stepped structural surface defects may explain the catalytic activity observed, and DFT calculation was employed to explore this possibility.

Fig. 5 presents the free energy for hydrogen adsorption on the terrace Au(111) (solid line) and few commonly studied stable stepped gold surfaces [53,54] (non-solid lines). The ΔG_{H^*} on the terrace Au(111) surface is calculated to be 0.45 eV following the work of Nørskov [16]. As shown, there are decreases of the ΔG_{H^*} on the stepped Au leading to a stronger bonding between hydrogen atom and the gold surface [39]. Gold is generally recognized to be a poor HER catalyst due to the weak adsorption of atomic hydrogen while a good HER catalyst should present a thermoneutral

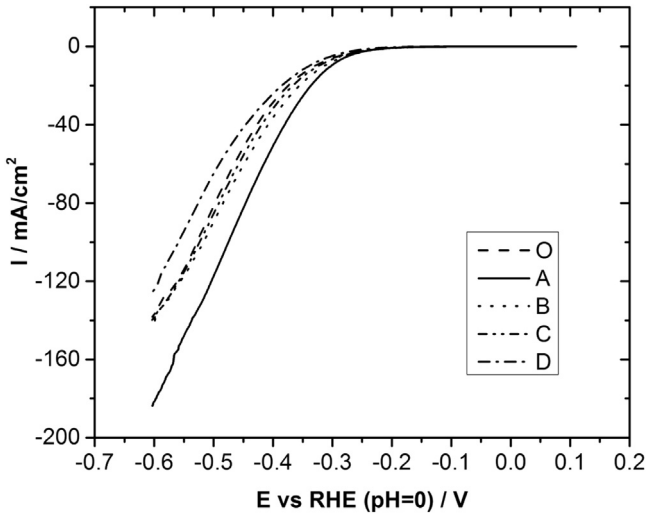

Fig. 4. The hydrogen evolution reaction in argon saturated 0.5 M sulfuric acid solution on bulk gold electrodes cycling with A: 0.64 V (—), B: 1.04 V (.....), C: 1.39 V (— · ·), D: 1. 74 V (– · –), and Original: without cycling (– –), 298 K, 100 mVs^{-1}.

adsorption free energy, that is to say $\Delta G_{H^*} = 0$ [55]. Hence, the reduced ΔG_{H^*} points out an enhanced adsorption of hydrogen atom on the stepped gold, which suggests a decrease of the energy barrier for the HER and this yields an electrocatalytic effect.

Several reasons can be considered for the inhibited electrochemical activity of HER on those under condition C and condition D. Firstly, the sluggish electrochemistry responses on both groups are in line with the reported disappearance of the step structures when the potential reaches 1.0 V vs SCE (1.24 V vs RHE) [45]. Secondly, Au-NPs/GCEs under condition D also experience a "RTO" (replacement turnover) process normally occurs after the OA1 peak shown in Fig. 2 [18,30,56]. This will lead to a more severe surface reconstruction process which might have an influence to the electrochemical response for inner-sphere electron transfer process like HER. Accordingly, the HER signal could be expected to be worse on Au-NPs/GCEs under condition D compared to that of condition C. Last but not least, the bigger particle size after the more aggressive cycling process with higher upper limit potential (See Fig. 6) might be another reason for the "negative" electrocatalytic effect. Size dependent electrocatalytic effect is not a new concept as it has found on many inner-sphere electron transfer systems, like CO_2 reduction [57] and the CO oxidation [58].

3.3. The Stability Test and Regeneration Experiment

The stability of the cycled Au nanoparticle catalysts was also investigated. As shown in Fig. 7a and b, the gross amount of the generated hydrogen and the generation rate are investigated and compared between the best performed Au-NPs/GCEs (condition A, open circles) and the Au-NPs/GCEs without cycling (open diamonds). In agreement with the former results, both the gross hydrogen production and generation rate are much larger on the Au-NPs/GCEs cycled under condition A. However, there is a remarkable drop of the generation rate for Au-NPs/GCE cycled under condition A in the first 30 minute displayed in Fig. 7b. Various factors might be blamed. Firstly, it could be the blocking of the active site owing to the strong adsorption of the accumulated intermediates generated during the proton reduction process. Secondly, the gold surface is well known to be reconstructed at negative potential. As reported, this surface is less active towards the HER compared to the one reconstructed at the positive potential [59]. Last but not least, these islands structures might experience a suppressing process with the increased amount of the generated hydrogen molecule which might destroys the "active" structure.

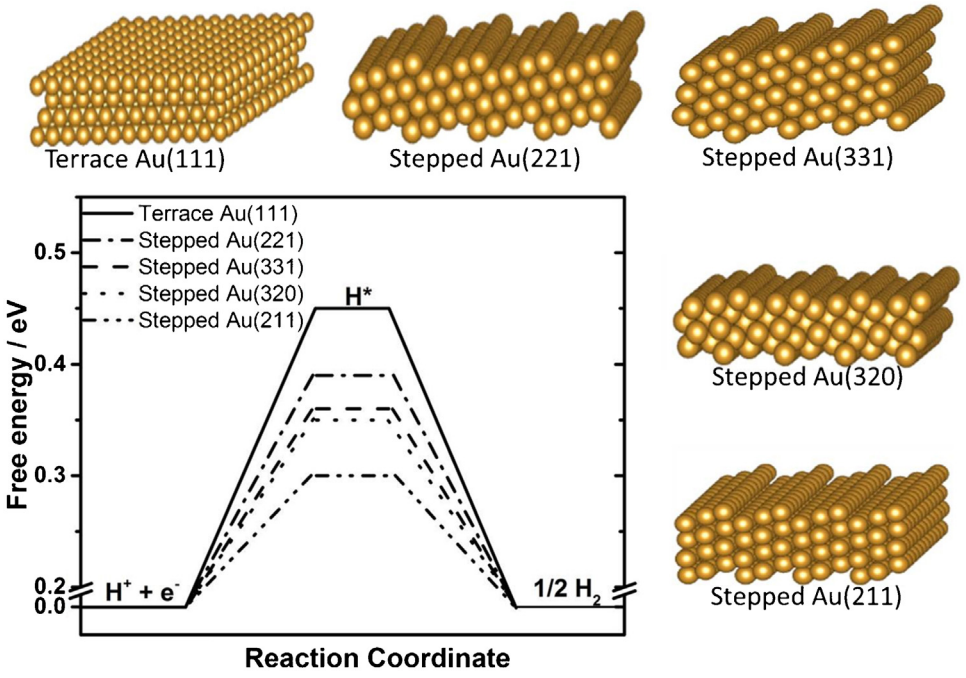

Fig. 5. Free energy diagram for the hydrogen evolution reaction on terrace Au surface (solid line) and Au with different stepped surfaces.

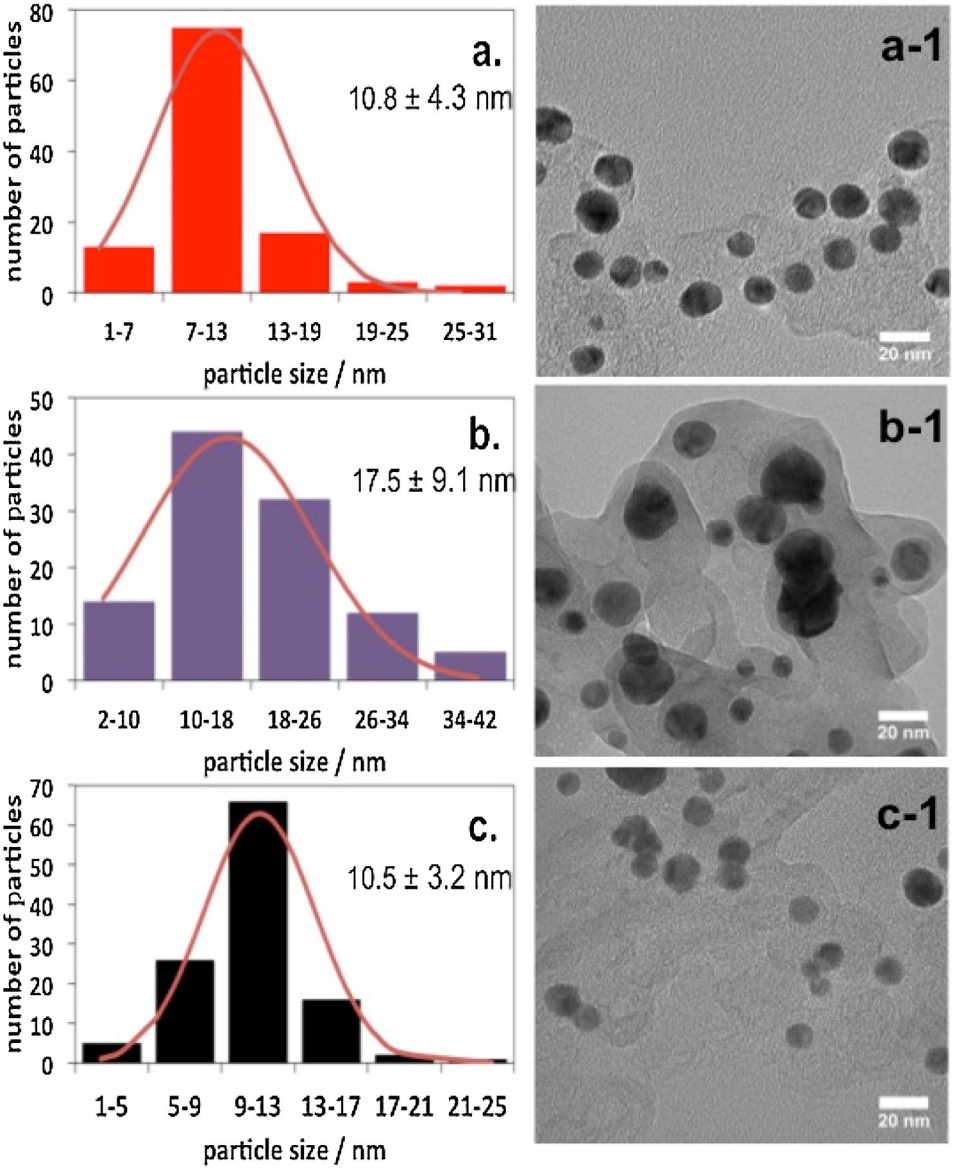

Fig. 6. Size distributions and TEM images for Au-NPs/GCE treated with upper limit potential of 0.64 V (a and a-1), 1.74 V (b and b-1) and without treatment (c and c-1). Noted that the results obtained are based on at least 100 nanoparticles.

Since the "modified gold electrode" will be deactivated in a short time period, we designed a regeneration protocol. The Au-NPs/GCEs were again electrochemically cycled for another 200 cycles under condition A after deactivation was observed. As it can be seen in Fig. 7c, the enhanced HER activity can be recovered after the electrochemical cycling process. The deactivation/regeneration cycle was repeated 6 times, with nearly complete recovery of the enhanced HER activity after the regeneration step. The recovery of the activity for the hydrogen evolution reaction shown in Fig. 7c suggests that the active structures can be reformed through electrochemical cycling process under condition A after the activity drop. Also, this further proves that the electrocatalytic effect observed in the group A is due to the "modification" from the electrochemical cycling process.

4. Conclusion

In summary, the electrochemical response of the HER can be altered on the Au-NPs/GCEs after electrochemical cycling with different upper limit potentials. The HER activity is enhanced on the gold nanoparticles after cycled with upper limit potential of 0.64 V vs RHE. The overpotential is 86.6 ± 10.9 mV which is 128 mV smaller than that on those without cycling process. A decreased Tafel slope of 76.6 ± 1.9 mV/dec is also obtained while it is 100.6 ± 5.0 mV/dec on the unmodified one. Additionally, this behaviour can be regenerated by electrochemically cycled in the same region after deactivation.

Acknowledgements

This work is supported by the MOE Tier 1 (RG13/13) and Tier 2 (MOE2015-T2-1-020) Grants of Singapore and by the Singapore National Research Foundation under its Campus for Research Excellence And Technological Enterprise (CREATE) programme though the Singapore-Berkeley Research Initiative for Sustainable Energy (SinBeRISE). We thank the Facility for Analysis, Characterisation, Testing and Simulation (FACTS) in Nanyang Technological University for materials characterization.

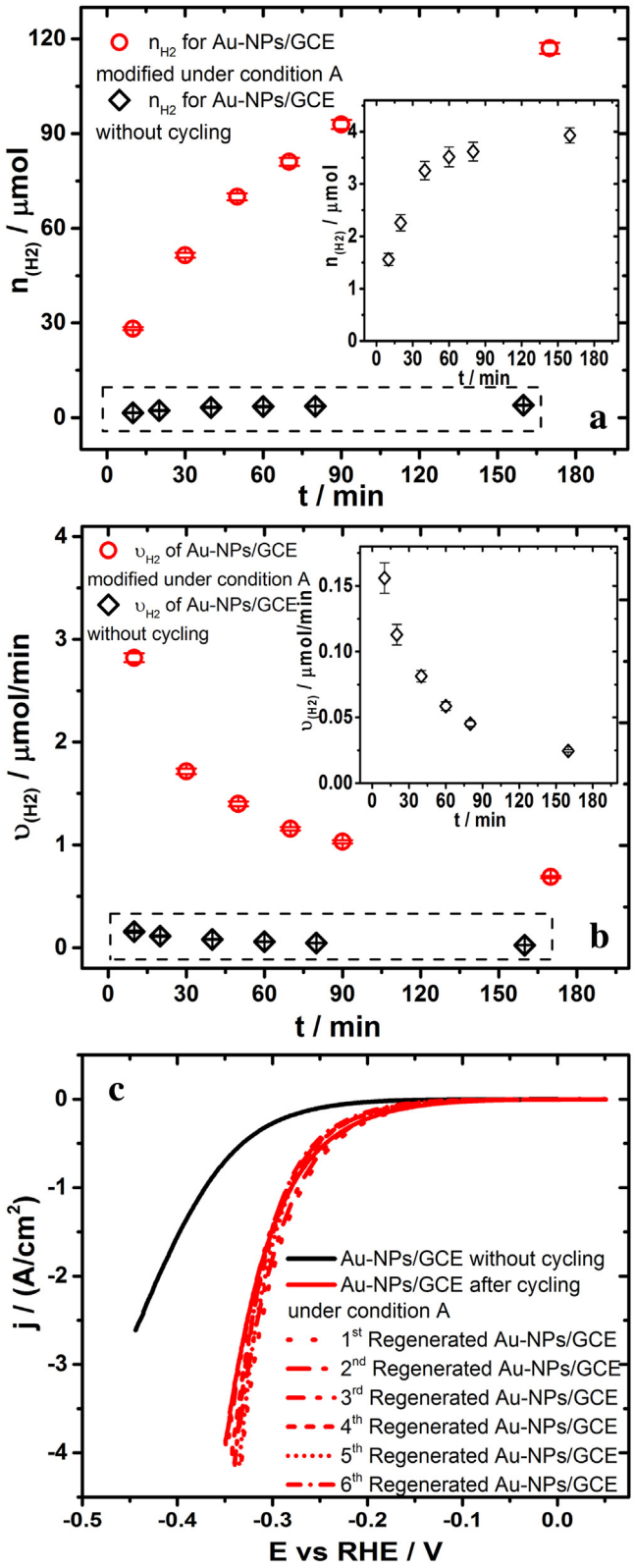

Fig. 7. Gross production (a) and generation rate of hydrogen (b) on Au-NPs/GCE cycled with upper limit potential of A: 0.64 V (open circle) and O: Au-NPs/GCE without cycling process (open diamond) at −0.31 V for 170 minutes in argon saturated 0.5 M sulfuric acid solution at 298 K, inserted are the enlarged dashed box region. (c) The regeneration of the Au-NPs/GCE.

References

[1] T.F. Jaramillo, K.P. Jørgensen, J. Bonde, J.H. Nielsen, S. Horch, I. Chorkendorff, Science 317 (2007) 100–102.
[2] W.F. Chen, K. Sasaki, C. Ma, A.I. Frenkel, N. Marinkovic, J.T. Muckerman, Y. Zhu, R.R. Adzic, Angewandte Chemie 51 (2012) 6131–6135.
[3] A.M. Gómez-Marín, K.J.P. Schouten, M.T.M. Koper, J.M. Feliu, Electrochemistry Communications 22 (2012) 153–156.
[4] J.D. Benck, T.R. Hellstern, J. Kibsgaard, P. Chakthranont, T.F. Jaramillo, ACS Catalysis 4 (2014) 3957–3971.
[5] Y. Fujimori, W.E. Kaden, M.A. Brown, B. Roldan Cuenya, M. Sterrer, H.-J. Freund, Journal of Physical Chemistry C 118 (2014) 17717–17723.
[6] C.G. Morales-Guio, L.A. Stern, X. Hu, Chemical Society Reviews 43 (2014) 6555–6569.
[7] E.J. Popczun, C.G. Read, C.W. Roske, N.S. Lewis, R.E. Schaak, Angewandte Chemie International Edition 53 (2014) 5427–5430.
[8] M. Smiljanic, Z. Rakocevic, A. Maksic, S. Strbac, Electrochimica Acta 117 (2014) 336–343.
[9] Y. Zheng, Y. Jiao, M. Jaroniec, S.Z. Qiao, Angewandte Chemie International Edition 54 (2015) 52–65.
[10] Y. Wang, E. Laborda, K. Tschulik, C. Damm, A. Molina, R.G. Compton, Nanoscale 6 (2014) 11024–11030.
[11] J.M. Bockris, International Journal of Hydrogen Energy 27 (2002) 731–740.
[12] J. Kibsgaard, T.F. Jaramillo, F. Besenbacher, Nature Chemistry 6 (2014) 248–253.
[13] J.A. Turner, Science 305 (2004) 972–974.
[14] W. Sheng, Z. Zhuang, M. Gao, J. Zheng, J.G. Chen, Y. Yan, Nature Communications 6 (2015) 5848.
[15] S. Shin, Z. Jin, H. Kwon do, R. Bose, Y.S. Min, Langmuir 31 (2015) 1196–1202.
[16] J.K. Nørskov, T. Bligaard, A. Logadottir, J. Kitchin, J. Chen, S. Pandelov, U. Stimming, Journal of the Electrochemical Society 152 (2005) J23–J26.
[17] M.S. El-Deab, T. Sotomura, T. Ohsaka, Electrochemistry Communications 7 (2005) 29–34.
[18] Y. Wang, E. Laborda, A. Crossley, R.G. Compton, Physical Chemistry Chemical Physics 15 (2013) 3133–3136.
[19] J. Zhang, K. Sasaki, E. Sutter, R.R. Adzic, Science 315 (2007) 220–222.
[20] P. Rodriguez, N. Garcia-Araez, A. Koverga, S. Frank, M.T.M. Koper, Langmuir 26 (2010) 12425–12432.
[21] G. Kresse, J. Furthmüller, Physical Review B 54 (1996) 11169.
[22] G. Kresse, D. Joubert, Physical Review B 59 (1999) 1758.
[23] Y. Zhang, W. Yang, Physical Review Letters 80 (1998) 890.
[24] H.J. Monkhorst, J.D. Pack, Physical Review B 13 (1976) 5188.
[25] A.A. Peterson, F. Abild-Pedersen, F. Studt, J. Rossmeisl, J.K. Nørskov, Energy & Environmental Science 3 (2010) 1311–1315.
[26] J.K. Nørskov, T. Bligaard, A. Logadottir, J. Kitchin, J. Chen, S. Pandelov, U. Stimming, Journal of Electrochemical Society 152 (2005) J23–J26.
[27] P. Atkins, Physical Chemistry, 6th ed., Oxford Press, Oxford, 1998.
[28] S.J. Xia, V.I. Birss, Journal of Electroanalytical Chemistry 500 (2001) 562–573.
[29] H. Angerstein-Kozlowska, B.E. Conway, K. Tellefsen, B. Barnett, Electrochimica Acta 34 (1989) 1045–1056.
[30] H. Angestein-Kozlowska, B.E. Conway, Electrochimica Acta 31 (1986) 1051–1061.
[31] J.C. Hoogvliet, M. Dijksma, B. Kamp, W.P. van Bennekom, Analytical Chemistry 72 (2000) 2016–2021.
[32] G. Tremiliosi-Filho, L.H. Dall'Antonia, G. Jerkiewicz, Journal of Electroanalytical Chemistry 422 (1997) 149–159.
[33] H. Angerstein-Kozlowska, B.E. Conway, B. Barnett, J. Mozota, Journal of Electroanalytical Chemistry 100 (1979) 417–446.
[34] A.P. O'Mullane, Nanoscale 6 (2014) 4012–4026.
[35] B.J. Plowman, N. Thompson, A.P. O'Mullane, Gold Bulletin 47 (2014) 177–183.
[36] D.M. Kolb, Electrochimica Acta 45 (2000) 2387–2402.
[37] M.A. Schneeweiss, D.M. Kolb, D. Liu, D. Mandler, Canadian Journal of Chemistry 75 (1997) 1703–1709.
[38] R.R. Adžić, S. Strbac, N. Anastasijević, Materials Chemistry and Physics 22 (1989) 349–375.
[39] H. Lv, Z. Xi, Z. Chen, S. Guo, Y. Yu, W. Zhu, Q. Li, X. Zhang, M. Pan, G. Lu, S. Mu, S. Sun, Journal of the American Chemical Society 137 (2015) 5859–5862.
[40] R.G. Compton, C.E. Banks, Understanding Voltammetry, World Scientific, 2007.
[41] M.S. Joohong Kye, Bora Lim, Jae-Won Jang, IIwhan Oh, Seongpil Hwang, ACS Nano 7 (2013) 6017–6023.
[42] J. Perez, E.R. Gonzalez, H.M. Villulas, Journal of Physical Chemistry B 102 (1998) 10931–10935.
[43] Y. Shi, J. Wang, C. Wang, T.-T. Zhai, W.-J. Bao, J.-J. Xu, X.-H. Xia, H.-Y. Chen, Journal of the American Chemical Society 137 (2015) 7365–7370.
[44] P. Xiao, M.A. Sk, L. Thia, X. Ge, R.J. Lim, J.-Y. Wang, K.H. Lim, X. Wang, Energy & Environmental Science 7 (2014) 2624–2629.
[45] R.J. Nichols, O.M. Magnussen, J. Hotlos, T. Twomey, R.J. Behm, D.M. Kolb, Journal of Electroanalytical Chemistry 290 (1990) 21–31.
[46] D.M. Kolb, Progress in Surface Science 51 (1996) 109–173.
[47] B. Pettinger, J. Lipkowski, S. Mirwald, A. Friedrich, Journal of Electroanalytical Chemistry 329 (1992) 289–311.
[48] Y. Wang, E. Laborda, K.R. Ward, K. Tschulik, R.G. Compton, Nanoscale 5 (2013) 9699–9708.
[49] A.A. Gewirth, B.K. Niece, Chemical Review 97 (1997) 1129–1162.
[50] D.V. Leff, C.P. Ohara, J.R. Heath, W.M. Gelbart, Journal of Physical Chemistry 99 (1995) 7036–7041.

[51] D. Kolb, J. Lipkowski, P.N. Ross, VCH, New York, 1993, pp. 65.
[52] K. Heinz, E. Lang, K. Strauss, K. Müller, Applications of Surface Science 11–12 (1982) 611–624.
[53] H. Mistry, R. Reske, Z. Zeng, Z.-J. Zhao, J. Greeley, P. Strasser, B.R. Cuenya, Journal of the American Chemical Society 136 (2014) 16473–16476.
[54] G.D. Barmparis, K. Honkala, I.N. Remediakis, Journal of Chemical Physics 138 (2013) 064702.
[55] D. Voiry, H. Yamaguchi, J. Li, R. Silva, D.C.B. Alves, T. Fujita, M. Chen, T. Asefa, V.B. Shenoy, G. Eda, M. Chhowalla, Nature Materials 12 (2013) 850–855.
[56] H. Angerstein-Kozlowska, B.E. Conway, A. Hamelin, L. Stoicoviciu, Journal of Electroanalytical Chemistry and Interfacial Electrochemistry 228 (1987) 429–453.
[57] R. Reske, H. Mistry, F. Behafarid, B. Roldan Cuenya, P. Strasser, Journal of the American Chemical Society 136 (2014) 6978–6986.
[58] B. Hvolbæk, T.V. Janssens, B.S. Clausen, H. Falsig, C.H. Christensen, J.K. Nørskov, Nano Today 2 (2007) 14–18.
[59] L.A. Kibler, Chemphyschem 7 (2006) 985–991.